Water Science & Technology

Water Science & Technology Vol 00 No 0, 1 doi: 10.2166/wst.2021.615

Treatment of the Allura Red food colorant contaminated water by a novel cyanobacterium *Desertifilum tharense*

Ülküye Dudu Gül [a,*], Zeynep Mine Şenol [b] and Burcu Ertit Taştan [c]

[a] Bilecik Seyh Edebali University, Faculty of Engineering, Department of Bioengineering, 11230, Bilecik, Turkey
[b] Cumhuriyet University, Zara Vocational School, 58140, Sivas, Turkey
[c] Gazi University, Health Services Vocational School, 06830, Gölbaşı, Ankara, Turkey
*Corresponding author. E-mail: ulkuyedudu.gul@bilecik.edu.tr

ÜDG, 0000-0001-6443-1633; ZMŞ, 0000-0002-5250-1267; BET, 0000-0003-4644-8305

ABSTRACT

The biosorption properties of a newly isolated and identified cyanobacterium called *Desertifilum tharense* were investigated in the current study. Following morphological and molecular identification (16S rRNA sequencing analysis), the food colorant removal potential of this new isolate was determined. Moreover, the isotherm, kinetic, and thermodynamic studies were performed, and also the biosorbent characterization was studied after and before colorant biosorption with Fourier transform infrared and scanning electron microscopy analysis. Additionally, the changes in chlorophyll content of the biosorbent were examined after and before colorant treatment. The newly isolated cyanobacterial biosorbent removed 97% of Allura Red food colorant/dye at 1,500 mg L^{-1} initial dye concentration successfully at optimal conditions. Langmuir isotherm and pseudo-second-order kinetic models were fitted with the biosorption of the dye. The D-R model showed that the biosorption process occurred physically. The chlorophyll-a content of the biosorbent was negatively affected by the biosorption. The newly isolated and identified cyanobacterium seems to be a successful candidate for use to treat highly dye concentrated wastewaters.

Key words: 16S rRNA sequencing analysis, Allura Red, biosorption, cyanobacteria, *Desertifilum tharense*, isolation

HIGHLIGHTS

- The food colorant removal performance of an isolated cyanobacterium identified with 16S rRNA sequencing as *Desertifilum tharense* was investigated.
- The maximum colorant biosorption capacity of algal biosorbent was very high.
- The biosorption process occurred physically.
- The sorption of colorant negatively affected the chlorophyll-a content of the cyanobacteria.

GRAPHICAL ABSTRACT

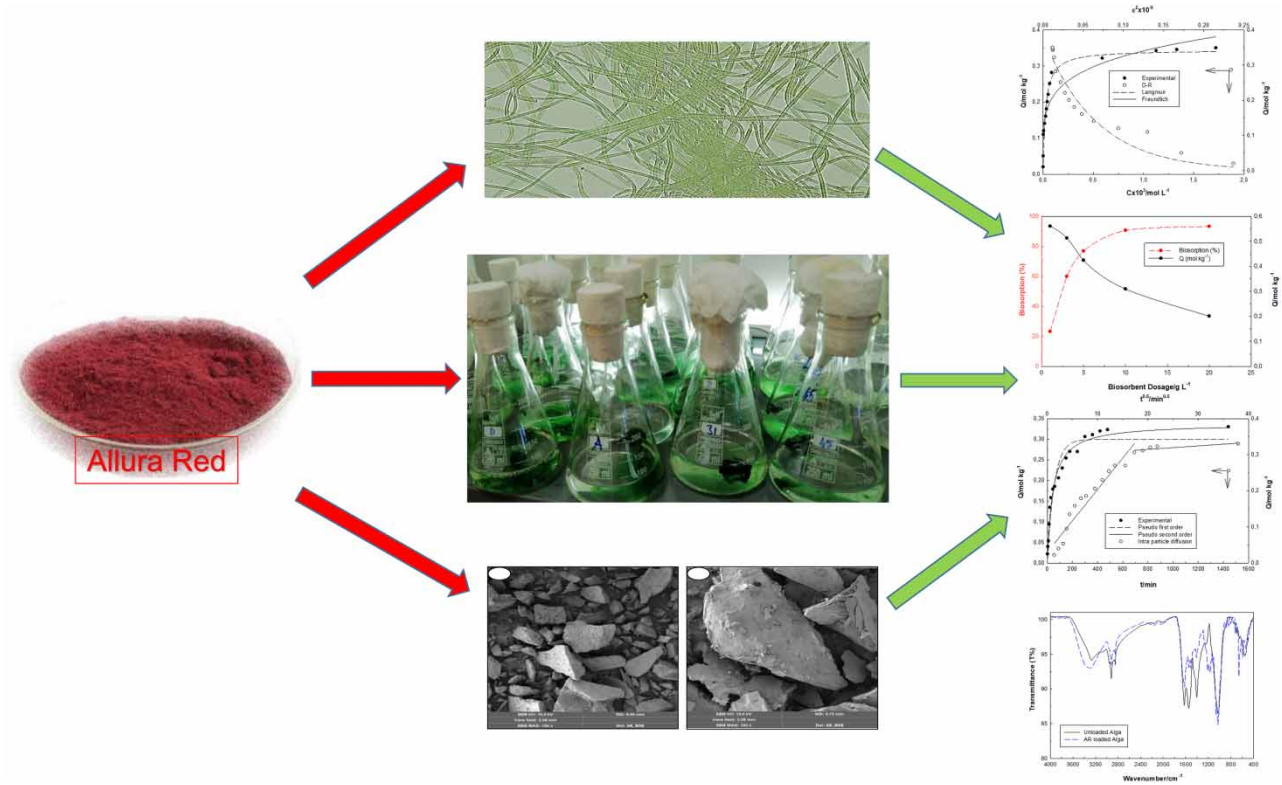

INTRODUCTION

Cyanobacteria are photosynthetic prokaryotes, also called blue-green algae, and at least 2,654 newly isolated species have been reported all over the world, extensively living in the water systems (Kenne & Merwe 2013). Members of the Cyanophyceae class have chlorophyll, which can convert sunlight energy into chemical energy (Barsanti & Gualtieri 2014). Recently, there has been an increased interest in studies on the usability of aquatic microorganisms such as cyanobacteria as biosorbent in environmentally friendly biological wastewater treatment technologies (Tastan *et al.* 2017; Kumar *et al.* 2019).

Allura Red (AR) is an extensively used colorant/dye in different industries such as food, medical, and cosmetics (Alkahtani *et al.* 2017), as well as most of the food coloring applications such as coloring bakery products, meat, and fish products, soft drinks, and jams (Al-Degs 2009).

Recent studies indicated that pollutants in wastewater released as a result of industrial activities harm aquatic organisms in water environments (Töre *et al.* 2021). Since the wastewater of these applications contains a high amount of colorants, which can be hazardous for aquatic organisms and eventually for humans, it is unavoidable to treat the colorant contaminated effluents (Nguyen *et al.* 2020; Majhi *et al.* 2021). Compared with chemical and physical treatment technologies, biological treatment technologies are preferred because of their eco-friendly nature (Mnif *et al.* 2016; Tastan & Tekinay 2016).

The main purpose of the study is to identify newly isolated cyanobacteria using 16S rRNA sequencing analysis, and then, to investigate the food colorant biosorption performance of newly isolated and identified cyanobacteria including isotherm, kinetic and thermodynamic studies. As a last objective, we intended to characterize the biosorbent before and after dye biosorption by Fourier transform infrared (FTIR) and scanning electron microscopy (SEM) analyses. Unlike other biosorption studies with the cyanobacterial originated biosorbent, the effect of the dye biosorption process on chlorophyll content was examined in the present study. The cyanobacterium called *Desertifilum tharense*, which was newly isolated from water samples in Turkey, was reported as the successful food colorant biosorption.

MATERIALS AND METHODS

Chemicals

The synthetic food colorant called Allura Red (AR) and all other chemicals were obtained from Merck (Germany). The stock solution was prepared by dissolving 200 mg of AR dye in 100 mL deionized water.

The isolation and cultural conditions of cyanobacteria

A novel cyanobacterium, which is used as a biosorbent to remove food colorant in water samples, was isolated from Denizli-Buharkent geothermal province located in Central Anatolia Region (Turkey).

In order to isolate cyanobacterial species from the water samples, BG11 agar-medium in the petri dishes was used (Rippka 1988). The samples were spread on the dishes and incubated under cool-white fluorescent, 25 μmol m_{-2} s_{-1} (1750 lx) light intensity at 25 ± 2 °C temperature. The medial pH was adjusted to 8 using either the solutions of sulfuric acid or sodium hydroxide (0.01 M and 1 M, respectively). The incubated microbial cells of the colonies were isolated with micromanipulation from the Petri dishes. At the aseptic conditions, the purification of cyanobacterial cells was performed by proceeding with the repeated inoculations on BG11 medium agar. After obtaining a pure culture, the cyanobacterial cells were inoculated into the liquid medium.

Polymerase chain reaction (PCR) and sequencing

The molecular identification method was applied to determine the new isolate. The genomic DNA was extracted from the cells harvested from an exponentially growing culture using *GenJet Genomic DNA Purification Kit*, according to the manufacturer's protocol. 16S rRNA is the elucidative region for isolate identification. The forward primer (106F: 5′-CGGACGGGTGAGTAACGCGTGA-3′) and the reverse primer (781R(a): 5′-GACTACTGGGGTATCTAATCCCATT-3′) were used to amplify the 16S rRNA region (Burja *et al.* 2001). The sequencing was performed in Applied Biosystems Genetic Analyzer 3130. The PCR reactions were carried out in a final volume of 50 μL containing 100 ng of purified DNA, 2.0 μL of $MgCl_2$ (2.0 mM), 1.5 U of Taq polymerase, and 0.3 μM of each forward and reverse primer. Amplifications were programmed on the thermocycler (Applied Biosystems Gene AMP PCR System 9700), at the following conditions: denaturation at 95 °C for 5 minutes, then 35 cycles of 1 minute at 94 °C, 1 minute at 60 °C, and 1 minute at 72 °C.

After all these processes the obtained sequences were compared to the reference sequences at National Center for Biotechnology Information (NCBI) by using an online program called The Basic Local Alignment Search Tool (BLAST 2020).

Preparation of cyanobacterial biomass

The pure culture of isolated *Desertifilum tharense,* a member of prokaryotic blue-green algae (cyanobacteria), was stored at the Culture Collection of Microalgae in Vocational School of Health Services, Gazi University, Ankara, Turkey. BG 11 culture medium (100 mL) was used for microalgal (cyanobacterial) incubation (Rippka 1988) in the Erlenmeyer flasks.

With the intention of large-scale microalgal (cyanobacterial) biomass production, sterile plastic reactors (with 5 L volume) containing BG11 were used. The application of dilute sodium hypochlorite and/or ethanol solutions was performed for sterilization. The motors with 8 W working capacity and 2–4 outputs were also administered for ventilation in the reactor system (Gül *et al.* 2019).

At the end of the exponential growth phase, the biomass was harvested using centrifugation (6,000 rpm, 5 min, 25 ± 2 °C) and dried at 70 °C overnight. The dried biomass was powdered by sieving with 0.5 mm pores and used in the biosorption assays. The experiments were carried out in triplicate and Equation (1) was used to calculate the specific growth rate (Ip & Chen 2005).

$$\mu = \ln x_2 - \ln x_1/t_2 - t_1 \quad (1)$$

where X_2 and X_1: dry cell weight concentrations (g/L) at time t_2 and t_1, respectively.

Biosorption experiments

The experiments were carried out as the batch scale method. The experimental systems are composed of solutions (deionized water) containing 100 mg of cyanobacterial biosorbent and 1,500 mg L^{-1} AR dye concentration at natural pH 8.5, for 24 h at 25 °C in polypropylene tubes (10 mL). The agitation speed of these systems was set up at 140 rpm at a thermostatic water bath. The pH effect was determined by using pH values varying from 1 to 12. The effect of the biosorbent dosage

was tested at 2–20 g L^{-1} biosorbent dosage. The concentrations of AR in solutions were determined spectrophotometrically at 506 nm (Uzcan & Soylak 2020). The AR concentrations were detected using a UV-Visible spectrophotometer (Shimadzu, 160 A model, Kyoto, Japan). Biosorption % and Q (mol kg^{-1}) were calculated by Equations (2) and (3).

$$\%\text{Biosorption} = [C_i - C_f/C_i] \times 100 \tag{2}$$

$$Q = [C_i - C_f/m] \times V \tag{3}$$

where, C_i is the initial concentration (mg L^{-1}), m refers to the adsorbent mass (g), C_f is equilibrium concentration (mg L^{-1}), and V is the solution volume (L).

Characterization of biosorbent

The surface zeta potentials (ZP) of biosorbents after and before biosorption were measured with the electrophoretic method by the usage of Malvern Zetasizer Nano ZS (Phoenix, EDAX, Mahwah, NJ, USA). The dispersant was deionized water with pH 8.5 (the pH value of experimental conditions). The biosorbent was characterized by analyses of FTIR and SEM. FTIR spectra of the biosorbents before and after biosorption of AR were measured in a Perkin Elmer 400 spectro photometer. SEM analysis was performed by using Leo 440 Computer Controlled Digital System.

Calculation of biosorption isotherms and kinetics

In this study, to gain detailed information about the biosorption mechanism, Langmuir, Freundlich, and Dubinin-Radushkevich isotherm models (Senol 2020) were used. The general equality of the Langmuir model is given in Equation (4).

$$Q = X_L K_L C_e/1 + K_L C_e \tag{4}$$

In this equation: Q (mol kg^{-1}): adsorbed amount, C_e (mol L^{-1}): equilibrium concentration, X_m: the maximum adsorption capacity of the adsorbent, K_L: dispersion coefficient

The equation of the Freundlich model is given in Equation (5).

$$Q = K_f C_e^{\beta} \tag{5}$$

In this equation: K_f: a measure of adsorption capacity, β: adsorbent surface heterogeneity

The Dubinin-Radushkevich (D-R) model, which examines the adsorption from the energetic point of view is given in Equation (6).

$$Q = Q_{DR} e_{DR}^{-K} \varepsilon^2 \tag{6}$$

In the D-R equation, the amount of adsorbed Q (mol kg^{-1}) is related to X_{DR}, a measure of adsorption capacity, activity coefficient K_{DR} (mol^2 KJ^2), and Polanyi potential (ε). Polanyi potential is calculated using Equation (7).

$$\varepsilon = RT\ln(1 + 1/C_e) \tag{7}$$

R is the ideal gas constant (8.314 J mol^{-1} K^{-1}) and T (K) is the absolute temperature. Adsorption energy (E) is calculated with Equation (8).

$$E = (2K_{DR})^{-0.5} \tag{8}$$

The value of E (kJ mol^{-1}) indicates whether the adsorption mechanism is physical or chemical. If the adsorption energy is $8<E<16$ kJ mol^{-1}, the adsorption is chemically controlled, and $E<8$ kJ mol^{-1} indicates that the adsorption proceeds physically.

Lagergren's pseudo-first-order (PFO) kinetic model, pseudo-second-order (PSO) kinetic model, and intra-particle diffusion (IPD) models were used to examine the biosorption kinetics. The equations were given as Equations (9)–(11) (Senol 2020) to

calculate Lagergren's pseudo-first-order model, pseudo-second-order kinetic model, and intraparticle diffusion model, respectively.

$$Q_t = Q_e(1 - e_1^{-kt}) \tag{9}$$

$$Q_t = t/[1/k_2Q_e^2] + [1/Q_e]t \tag{10}$$

$$Q_t = k_i t^{0.5} \tag{11}$$

In these equations: Qt (mol kg^{-1}) is the number of ions in the moment of t and Q_e (mol kg^{-1}) is the amount of ion in the equilibrium. k_1 (min^{-1}) and k_2 (mol kg min^{-1}) show first- and second-order rate constants, respectively. The initial speeds for the pseudo-first- and second-order models of adsorption are calculated by Equations (12) and (13), respectively (Senol 2020).

$$H_1 = k_1Q_e \tag{12}$$

$$H_2 = k_2Q_e^2 \tag{13}$$

Analysis of cyanobacterial morphology

In order to gain information about the cyanobacterial morphology, the living cyanobacterial biomass was viewed under a microscope (Zeiss-Primo Star). The morphological properties of the cyanobacterium were investigated as well.

Analysis of the changes in cyanobacterial physiology

In the previous studies, chlorophyll a, chlorophyll b, and chlorophyll (a + b) contents were frequently examined to evaluate the change in the physiological state of lichen (a symbiotic lifestyle of a fungus as mycobiont and an alga or a cyanobacterium as photobiont) under various environmental stress conditions (Boonpragob 2002). However, little is known about the effect of textile dye on chlorophyll concentration in photosynthetic organisms such as algae (Copaciu *et al.* 2013; Rane *et al.* 2014). *D. tharense* is a filamentous cyanobacterium (Oscillatoriales), with a trichome width size of 2–3.7 μm in diameter (Dadheech *et al.* 2012). The chlorophyll concentration of *D. tharense* was determined according to the method developed by Porra *et al.* (1989) at 646.6 nm for chlorophyll *a*. The chlorophyll concentrations were expressed in μg of chlorophyll per milliliter.

RESULTS AND DISCUSSION

A newly isolated blue-green alga (cyanobacterium) was identified by molecular techniques and then the food colorant removal properties of this microorganism were investigated. The calculation of biosorption isotherms and kinetics, and also biosorbent characterization studies such as ZP, FTIR, and SEM before and after the biosorption process were carried out. Also, the changes in cyanobacterial physiology after the biosorption process were examined.

Identification and morphology of the new isolate

According to the information obtained from the BLAST program, the new cyanobacteria isolate was identified as *Desertifilum tharense* from 16S rRNA sequencing. The classification of this species is also submitted in Supplementary material 1 (Dadheech *et al.* 2012).

The morphology of the cyanobacterium was observed under the light microscope and the micrograph of the cyanobacterium is given in Figure 1. While the morphology of *D. tharense* was investigated, the cyanobacterial biomass had a multicellular filamentous structure similar to other species belonging to the order *Oscillatoriales* (Martins & Branco 2016). The morphological characteristics of the isolated cyanobacterium were observed as having thin thallus, densely entangled filaments, agglutinated trichomes, and cylindrical cells having homogeneous content (Figure 1). The cell wall lies between the plasma membrane and the mucilaginous sheet and the filaments were simple, which was previously explained for the appearance of other cyanobacterial cells by Barsanti & Gualtieri (2014). Similarly, Dadheech *et al.* (2012) isolated a cyanobacterium strain from Rajasthan, India, and identified this cyanobacterium as *Desertifilum tharense*. The cyanobacterium species newly isolated in this study showed a similar morphology identified by Dadheech *et al.* (2012). The algae/cyanobacteria had a characteristic green color due to the pigment Chlorophyll-a, which was responsible for photosynthesis (Sinetova *et al.* 2017).

Figure 1 | The microscobic image of *Desertifilum tharense (400 x)*.

Effect of pH on biosorption of AR food dye

The effect of pH was examined via the variety of pH values from 1.0 to 12.0 and as seen in Figure 2. The decolorization rate was not significantly changed from pH 4.0 to 8.5. The pHs at the point of zero charges (pHpzc) of blue-green algal strains were reported in the range of 4.6–8.5 in the literature (Martinez *et al.* 2008; Mishra & Mukherji 2012; Dotto *et al.* 2013). Similarly, the colorant biosorption rate was sharply decreased after pH 8.5 due to the pHpzc of the cyanobacterium strain (Figure 2(a)). The optimal pH was selected as 8.5 in the present study.

Effect of biosorbent dosage on biosorption of AR food dye

The effect of cyanobacterial biosorbent dosage on food colorant biosorption was tested with a variety of biosorbent closes in the range of 10–200 mg. The increase of biosorbent dosage caused the augmentation of the dye biosorption rate. Recently, Gül *et al.* (2019) showed that acid red textile dye biosorption of another algal species called *Phormidium animale* was increased by the increment of dye concentration. Similarly, Bayazit *et al.* (2020) reported that Remazol Black B textile dye removal by *P.*

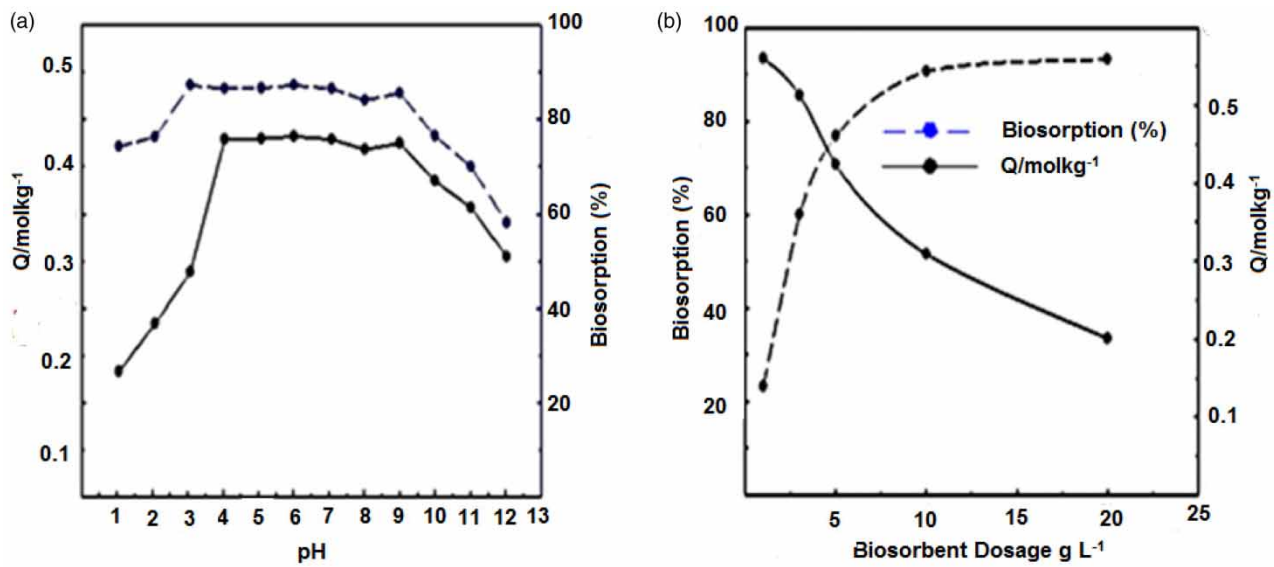

Figure 2 | (a) Effect of pH on biosorption of AR food dye onto cyanobacterial biosorbent ($[AR]_0$=1,500 mg L^{-1}, biosorbent dosage=100 mg, V=10 mL, pH=1.0–12.0, contact time: 24 h, temperature: 25 °C), (b) Effect of biosorbent dosage on biosorption of AR food dye onto cyanobacterial biosorbent ($[AR]_0$=1,500 mg L^{-1}, biosorbent dosage=10, 30, 50, 100, 200 mg, V=10 mL, pH=8.5, contact time: 24 h, temperature: 25 °C).

animale biosorbent was raised with the increasing biosorbent dosage. These increasing patterns were explained by the raising of available biosorption sites on the surface of the biosorbent (Saeed *et al.* 2010). The maximum AR biosorption was found 97% with 200 mg biosorbent dosage in a 10 ml working solution (Figure 2(b)).

Biosorption isotherm models

In order to obtain more detailed information about the biosorption of AR by cyanobacterial biosorbent, the biosorption isotherm models were derived from the biosorption experiments. The graphs of biosorption isotherm models are given in Supplementary material 2.

The calculations of R^2 values from Langmuir and Freundlich biosorption isotherm models showed that biosorption of food colorant AR was fitted with the Langmuir isotherm model (Table 1). The maximum biosorption capacity was found to be 0.345 mol kg^{-1}, and the biosorption energy was found to be 5.73 kJ mol^{-1}, which indicated that the biosorption process was physical.

Biosorption kinetics

The experimental data was used to understand the fitted kinetic model for biosorption (Supplementary material 3). In the experimental series, it was observed that the biosorption process was stabilized after 420 minutes. According to the results of kinetic calculations, the biosorption process was better adapted to the pseudo-second-order kinetic model due to the correlation coefficients (Table 2).

At the same time, when the experimentally calculated Q_t values and the theoretically calculated Q_e values were compared, the results found from the pseudo-second-order kinetic model were found to be closer to each other. These results indicated that the biosorption process followed the pseudo-second-order kinetics.

Biosorption thermodynamic

The effect of temperature on the food colorant by cyanobacterial biosorbent was determined at 5 °C, 25 °C, and 40 °C. The increasing temperature caused decreasing biosorption rate (Supplementary material 4), which was reported as a characteristic phenomenon of physical adsorption (Aksu & Tezer 2005). And this situation also supported the results of D-R

Table 1 | Langmuir, Freundlich and Dubinin-Radushkevich isotherm model parameters

Langmuir			Freundlich			Dubinin-Radushkevich			
X_L	K_L	R^2	K_f	β	R^2	X_{DR}	$K_{DR}\times10^9$	E_{DR}	R^2
0.345	39690	0.956	1.36	0.200	0.870	0.381	1.52	5.73	0.929

X_L (mol kg^{-1}), K_L (L mol^{-1}), X_{DR} (mol kg^{-1}), $K_{DR} \times 10^9$ (mol^2KJ^{-2}), E_{DR} (kJ mol^{-1}).

Table 2 | Kinetic model parameters

Pseudo-first-order kinetic				
Q_t/(molkg^{-1})	Q_e/(molkg^{-1})	R^2	$k_1\times10^3$/(dk^{-1})	$H\times10^3$/(mol kg^{-1} min^{-1})
0.330	0.300	0.942	18.0	5.41
Pseudo-second-order kinetic				
Q_t/(molkg^{-1})	Q_e/(molkg^{-1})	R^2	$k_2\times10^3$/(mol^{-1}kgmin^{-1})	$H\times10^3$/(mol kg^{-1} min^{-1})
0.330	0.338	0.982	69.2	7.91
Intraparticle diffusion				
–	–	R^2	$k_i\times10^3$/(mol kg^{-1} min$^{-0.5}$)	–
–	–	0.927	30.0	–

Table 3 | Adsorption thermodynamic parameters

ΔH^0/kJ mol^{-1}	ΔS^0/J mol^{-1} K^{-1}	ΔG^0/kJ mol^{-1}	R^2
27.8	158	−19.3	0.999

calculations derived in this study. The calculations of biosorption thermodynamics showed that the biosorption of food colorant by cyanobacterial biosorbent was endothermic, entropy increased, and spontaneous (Table 3).

ZP and SEM analysis

To have more detailed information about the colorant and biosorbent interactions, ZP and SEM analyses were performed. The surface zeta potentials (E_{zeta}) of the cyanobacterial biosorbents before and after biosorption were measured as 0.226 and 0.140 mV at pH 8.5 (the pH of experimental conditions), respectively. After the AR biosorption process, the positively charged value of the biosorbent was decreased due to the negative charge of the anionic dye. The change in the E_{zeta} indicated the sorption of dye molecules onto the surface of the cyanobacterial biosorbent. In Figure 2(a), the colorant removal decreased sharply after pH 8.5 due to the changes in surface charge of the cyanobacterial biosorbent. Similarly, the pH values at the isoelectric point of *Anabaena varialis* and *Prochlotrix hollandica*, which were also filamentous cyanobacteria, were measured as 8.4 and 8.1, respectively (Davis *et al.* 1980; Babu *et al.* 1999). It is known that pH is the most important factor affecting the zeta potential of the cell surface (Martinez *et al.* 2008). It is assumed that while the pH increased from 8.5 to 12, the zeta potential was changed due to the isoelectric point of zero, which resulted in a decrease in decolorization.

The SEM micrographs of dried cyanobacterial biosorbent before and after the biosorption process are given in Figure 3(a) and 3(b), respectively. Recently, Hussein *et al.* (2018) reported that the surface morphology of a filamentous blue-green alga (Cyanobacterium) called *Nostoc carneum* was changed depending on the sorption of Methyl Orange dye after the biosorption process. Similarly, in this study, the surface morphology of the cyanobacterial biosorbent of *D. tharense* seems different after and before biosorption. The surface of cyanobacterial biomass was irregular and porous before biosorption (Figure 3(a)). After

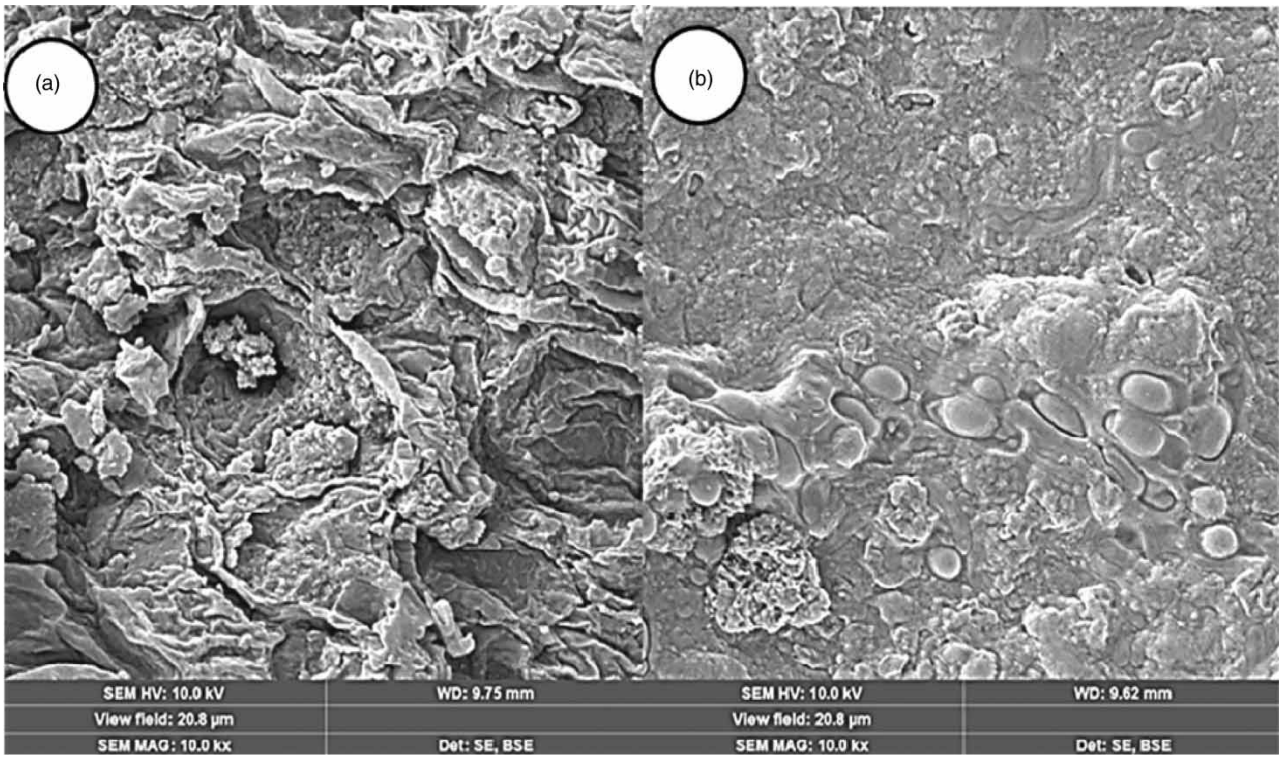

Figure 3 | SEM micrographs of dried cyanobacterial biosorbent before (a) and after (b) biosorption.

biosorption, the biomass particles were densely packed due to the presence of dye molecules that made a monolayer on the surface. A similar situation was shown by Kumar *et al.* 2019, who studied the biosorption of Orange G dye by the dried powdered algal biomass called *Chlorella vulgaris*. Also, Kiran *et al.* (2016) explained that the algal surfaces have a high affinity to the pollutants to form monolayers, which caused aggregations of the algal biomass. The SEM results of this study fitted with the recently published articles in the literature.

FTIR analysis

Fourier transform infrared (FTIR) analysis is a kind of vibrational spectroscopy, and the FTIR spectra reflect the changes of functional groups on the surface of cyanobacterial biomass after the biosorption process. The changes on the peaks before and after biosorption indicated the functional groups which were responsible for the colorant sorption (Figure 4). The peaks observed at 2,917.24 and 2,919.02 cm^{-1} (before and after) corresponded to the C–H stretching vibration. The peak that appeared at 1,625.95 cm^{-1} shifted to 1,620.39 cm^{-1} after colorant sorption, indicating the involvement of C-O stretching in the biosorption process (Bhattacharya *et al.* 2014). The peak which appeared in the region of 1,546.92 cm^{-1} represented protein amide II band (mainly δ(N-H) bending) on the surface of algal biomass (Theivandran *et al.* 2015), which disappeared after biosorption. The new peak at 1,174.60 cm^{-1} occurring after biosorption, which was found in the frequency ranges of 1,250–1,020 cm^{-1}, represented the C–N s stretching vibration presence of aliphatic amines (Mona *et al.* 2011b). Also similarly, the peak at 1,024.48 cm^{-1} before biosorption shifting to 1,032.04 cm^{-1} after biosorption revealed the C–N s stretching. These changes on the surface functional groups of algae or cyanobacteria showed that there were some interactions between the surface of algal biosorbent and the colorant molecules after the biosorption process. The results of FTIR showed that the functional groups like hydroxyl, amide, and carboxylate groups found on the surface of cyanobacterial cells were mainly responsible for the biosorption of food colorant.

The ZP, SEM, and FTIR analysis indicated the adsorption of the colorant molecules on the surface of the biosorbent, and the thermodynamic and D-R model results showed that the biosorption occurred physically.

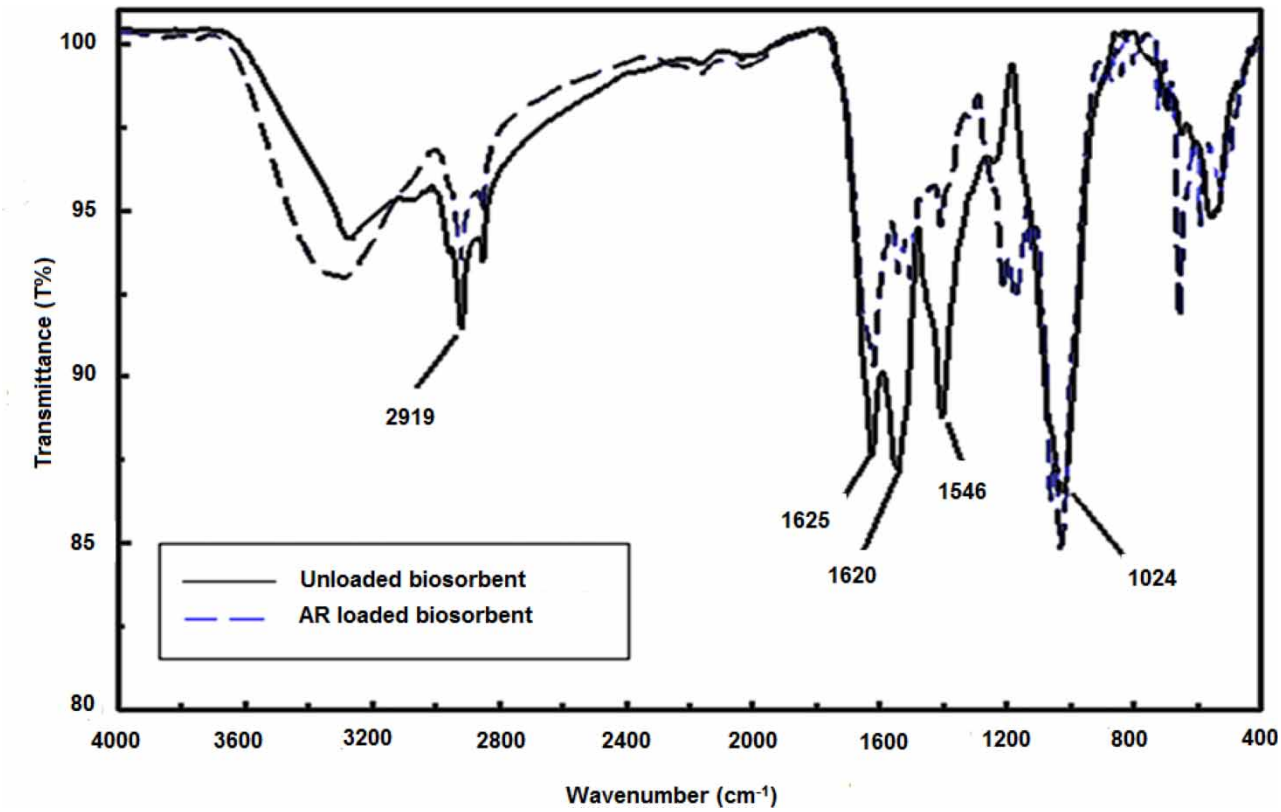

Figure 4 | FT-IR spectrum of unloaded and AR loaded cyanobacterial biosorbent.

Table 4 | The comparison of cyanobacterial or algal biosorbents among their decolorization performances (C_o: Initial dye concentration (mg L^{-1}); BD: Biosorbent dosage; D%: Decolorization percentage)

Algal species	Dye	pH	C_o	BD	T	D%	Reference
Chlorella vulgaris	Remazol Black B	2.0	86.3	1 gL^{-1}	35	63.00	Aksu & Tezer (2005)
Chlorella vulgaris	Remazol Red	2.0	75.1	1 gL^{-1}	25	73.60	Aksu & Tezer (2005)
Nostoc linckia	Crystal violet	8.0	200	0.2 g	35	72.00	Mona *et al.* (2011a)
Nostoc linckia HA 46	Reactive Red 198	2.0	100	–	35	94.00	Mona *et al.* (2011b)
Phormidium animale	Acid red	2.0	100	4 gL^{-1}	45	99.07	Gül *et al.* (2019)
Chlorella vulgaris	Orange 6	5.0	5	50 mg	10	44.00	Kumar *et al.* (2019)
Phormidium animale	Remazol Black B	2.0	93.16	4 gL^{-1}	45	99.66	Bayazit *et al.* (2020)
Desertifilum tharense	Allura Red	8.5	1,500	200 mg	25	97.00	in the present study

Changes in cyanobacterial physiology

The cyanobacterial biomasses were used as biosorbents for the removal of dye molecules (Mona *et al.* 2011a, 2011b; Gül *et al.* 2019; Bayazit *et al.* 2020). According to our best knowledge, there is no study to determine the relationship between dye molecules and the chlorophyll content of cyanobacterium. The chlorophyll-a concentration of dried *D. tharense* culture was 3.7 μg mL^{-1} before AR colorant biosorption. This concentration decreased to 3.06 μg mL^{-1} after AR colorant biosorption onto the cyanobacterium biomass. It is assumed that the decrease of chlorophyll-a content indicated the interaction of dye molecules with chlorophyll-a on the surface of the cyanobacterium, and therefore the sorption of dye molecules affects the amount of chlorophyll-a.

The comparison of cyanobacterial or algal biosorbents

In the last studies, the usage of cyanobacterial biomasses as the low-cost and eco-friendly biosorbents to remove a variety of dye molecules from wastewaters was investigated. Some of these studies about cyanobacterial or algal dye biosorption were reviewed and the results are given in Table 4. As seen in Table 4, our newly isolated cyanobacterial biomass called *D. tharense* performed a very successful decolorization rate at the highest initial dye concentration of 1,500 mg L^{-1}.

CONCLUSION

Industrial wastewaters contain varying concentrations of dyestuffs. Despite the high decolorization efficiency of some strains, they may fail to remove dyes and some environmental problems may arise. The biosorbent originated from *D. tharense* removed 97% of AR dye from an aqueous solution containing a high concentration of the dye (1,500 mg L^{-1}). According to our present knowledge, there isn't any study focusing on the dye biosorption potential of *D. tharense* identified in this study. The reviewed literature about dye removal by cyanobacterial or algal biosorbents (Table 4) showed that the identified cyanobacteria *D. tharense* in the present study performed dye removal capacity at approximately 10 times higher dye concentration than other biosorbents obtained from cyanobacteria or algae. The results of isotherm, kinetic, thermodynamic calculations, and characterization studies (FTIR and SEM) supported that the food colorant molecules physically adsorbed on the surface of biosorbent (*D. tharense* originated). It is concluded that the identified novel cyanobacterium was a useful candidate to remove high concentrations of food colorants from wastewater according to this preliminary lab-scale study. Further pilot-scale studies may show the utilization of this biosorbent in wastewater treatment plants.

DATA AVAILABILITY STATEMENT

All relevant data are included in the paper or its Supplementary Information.

REFERENCES

Aksu, Z. & Tezer, S. 2005 Biosorption of reactive dyes on the green alga *Chlorella vulgaris*. *Process Biochemistry* **40**, 1347–1361. https://doi.org/10.1016/j.procbio.2004.06.007.

Al-Degs, Y. 2009 Determination of three dyes in commercial soft drinks using HLA/GO and liquid chromatography. *Food Chemistry* **117** (3), 485–490. https://doi.org/10.1016/j.foodchem.2009.04.097.

Alkahtani, S. A., Abu-Alrub, S. S. & Mahmoud, A. M. 2017 Adsorption of food coloring allura red dye (E129) from aqueous solutions using activated carbon. *International Journal of Food and Allied Sciences* **3** (1), 10–19. https://doi.org/10.21620/ijfaas.2017110-26.

Babu, C. R., Volkman, B. F. & Bullerjahn, G. S. 1999 NMR solution structure of plastocyanin from the photosynthetic prokaryote, *Prochlorothrix hollandica*. *Biochemistry* **38** (16), 4988–4995. https://doi.org/10.1021/bi983024f.

Barsanti, L. & Gualtieri, P. 2014 *Algae: Anatomy, Biochemistry, and Biotechnology*, 2nd edn. CRC Press Taylor & Francis Group, Boca Raton, FL, p. 361. https://doi.org/10.1201/b16544. ISBN 978-1-4398-6732-7.

Bayazit, G., Tastan, B. E. & Gül, Ü. D. 2020 Biosorption, isotherm, and kinetic properties of common textile dye by *Phormidium animale*. *Global Nest Journal* **22** (1), 1–7. https://doi.org/10.30955/gnj.002984.

Bhattacharya, P., Mallick, K., Ghosh, S., Banerjee Mukhopadhyay, P. A. & Bandyopadhyay, S. 2014 Algal biomass as potential biosorbent for reduction of organic load in gray water and subsequent reuse: effect on seed germination and enzyme activity. *Bioremediation Journal* **18** (1), 56–70. https://doi.org/10.1080/10889868.2013.847400.

BLAST 2020. Available from: http://blast.ncbi.nlm.nih.gov/Blast.cgi (04.15.2020)

Boonpragob, K. 2002 Monitoring physiological change in lichens: total chlorophyll content and chlorophyll degradation. In: *Monitoring with Lichens – Monitoring Lichens. NATO Science Series (Series IV: Earth and Environmental Sciences)* (Nimis, P. L., Scheidegger, C. & Wolseley, P. A., eds). Springer, Dordrecht, p. 7. https://doi.org/10.1007/978-94-010-0423-7_28

Burja, A. M., Tamagnini, P., Bustard, M. T. & Wright, P. C. 2001 Identification of the green alga, *Chlorella vulgaris* (SDC1) using cyanobacteria derived 16S rDNA primers: targeting the chloroplast. *FEMS Microbiology Letters* **202**, 195–203. https://doi.org/10.1111/j.1574-6968.2001.tb10803.x.

Copaciu, F., Opris, O., Coman, V., Ristoiu, D., Niinemets, Ü. & Copolovici, L. 2013 Diffuse water 226 pollution by anthraquinone and azo dyes in environment importantly alters foliage volatiles, 227 carotenoids and physiology in wheat (*Triticum aestivum*). *Water Air and Soil Pollution* **224**, 1478. https://doi.org/10.1007/s11270-013-1478-4.

Dadheech, P. K., Abed, R. M. M., Mahmoud, H., Mohan, M. K. & Krienitz, L. 2012 Polyphasic characterization of cyanobacteria isolated from desert crusts, and the description of *Desertifilum tharense* gen. et sp. nov. (Oscillatoriales). *Phycologia* **51**, 260–270. https://doi.org/10.2216/09-51.1.

Davis, D. J., Krogmann, D. W. & Pietro, A. S. 1980 Electron donation to photosystem 1. *Plant Physiology* **65** (4), 697–702. https://doi.org/10.1104/pp.65.4.697.

Dotto, G. L., Vieira, M. L. G., Esquerdo, V. M. & Pinto, L. A. A. 2013 Equilibrium and thermodynamics of azo dyes biosorption on to *Spirulina platensis*. *Brazilian Journal of Chemical Engineering* **30** (01), 13–21. https://doi.org/10.1590/S0104-66322013000100003.

Gül, Ü. D., Tastan, B. E. & Bayazit, G. 2019 Assessment of algal biomasses having different cell structures for biosorption properties of acid red P-2BX dye. *South African Journal of Botany* **127**, 147–152. https://doi.org/10.1016/j.sajb.2019.08.047.

Hussein, M. H., Abou El-Wafa, G. S., Shaaban-Dessuki, S. A. & El-Morsy, R. M. 2018 Bioremediation of methyl orange onto *Nostoc carneum* biomass by adsorption; kinetics and isotherm studies. *Global Advanced Research Journal of Microbiology* **7** (1), 006–022.

Ip, P. F. & Chen, F. 2005 Production of astaxanthin by the green microalga *Chlorella zofingiensis* in the dark. *Process Biochemistry* **40** (2), 733–738. https://doi.org/10.1016/j.procbio.2004.01.039.

Kenne, G. & Merwe, D. 2013 Classification of toxic cyanobacterial blooms by Fourier-transform infrared technology (FTIR). *Advances in Microbiology* **3** (6), 1–8.

Kiran, B., Rani, N. & Kaushik, A. 2016 FTIR spectroscopy and scanning electron microscopic analysis of pretreated biosorbent to observe the effect on Cr (VI) remediation. *International Journal of Phytoremediation* **18**, 1067–1074. https://doi.org/10.1080/15226514.2016.1183577.

Kumar, S., Ahluwalia, A. S. & Charaya, M. U. 2019 Adsorption of Orange-G dye by the dried powdered biomass of *Chlorella vulgaris* Beijerinck. *Current Science* **116** (4), 604–611. https://doi.org/10.18520/cs/v116/i4/604-611.

Majhi, P. K., Kothari, R., Arora, N. K., Pandey, V. C. & Tyagi, V. V. 2021 Impact of pH on pollutional parameters of textile industry wastewater with use of *Chlorella pyrenoidosa* at lab-scale: a green approach. *Bulletin of Environmental Contamination and Toxicology*. https://doi.org/10.1007/s00128-021-03208-5.

Martinez, R. E., Pokrovsky, O. S., Schott, J. & Oelkers, E. H. 2008 Surface charge and zeta-potential of metabolically active and dead cyanobacteria. *Journal of Colloid and Interface Science* **323** (2), 317–325. https://doi.org/10.1016/j.jcis.2008.04.041.

Martins, M. D. & Branco, L. H. Z. 2016 Potamolinea gen. nov. (Oscillatoriales, Cyanobacteria): a phylogenetically and ecologically coherent cyanobacterial genus. *International Journal of Systematic and Evolutionary Microbiology* **66** (9), 3632–3641. https://doi.org/10.1099/ijsem.0.001243.

Mishra, P. K. & Mukherji, S. 2012 Biosorption of diesel and lubricating oil on algal biomass. *3 Biotech* **2**, 301–310. https://doi.org/10.1007/s13205-012-0056-6.

Mnif, I., Maktouf, S., Fendri, R., Kriaa, M., Ellouze, S. & Ghribi, D. 2016 Improvement of methyl orange dye biotreatment by a novel isolated strain, *Aeromonas veronii* GRI, by SPB1 biosurfactant addition. *Environmental Science and Pollution Research* **23**, 1742–1754. (2016). https://doi.org/10.1007/s11356-015-5294-9.

Mona, S., Kaushik, A. & Kaushik, C. P. 2011a Waste biomass of *Nostoc linckia* as adsorbent of crystal violet dye: optimization based on statistical model. *International Biodeteriation and Biodegradation* **65**, 513–521. https://doi.org/10.1016/j.ibiod.2011.02.002.

Mona, S., Kaushik, A. & Kaushik, C. P. 2011b Biosorption of reactive dye by waste biomass of *Nostoc lincki*. *Ecological Engineering* **37** (10), 1589–1594. https://doi.org/10.1016/j.ecoleng.2011.04.005.

Nguyen, T. Q., Sesin, V., Kisiala, A. & Neil Emery, R. J. 2020 The role of phytohormones in enhancing metal remediation capacity of algae. *Bulletin of Environmental Contamination and Toxicology* **105**, 671–678. https://doi.org/10.1007/s00128-020-02880-3.

Porra, R. J., Thompson, W. A. & Kreidemann, P. E. 1989 Determination of accurate extinction coefficients and simultaneous equations for assaying chlorophylls a and b extracted with four different solvents: verification of the concentration of chlorophyll standards by atomic absorption spectroscopy. *Biochimica Biophysica Acta* **975** (3), 384–394. https://doi.org/10.1016/S0005-2728(89)80347-0.

Rane, N. R., Chandanshive, V. V., Khandare, R. V., Gholave, A. R., Yadav, S. R. & Govindwar, S. P. 2014 Green remediation of textile dyes containing wastewater by *Ipomoea hederifolia*. *RSC Advantages* **4**, 36623–36632. https://doi.org/10.1039/C4RA06840H.

Rippka, R. 1988 Recognition and identification of cyanobacteria. *Methods in Enzymology* **167**, 28–67. https://doi.org/10.1016/0076-6879(88)67005-4.

Saeed, A., Sharif, M. & Iqbal, M. 2010 Application potential of grapefruit peel as dye sorbent: kinetics, equilibrium, and mechanism of crystal violet adsorption. *Journal of Hazardous Materials* **179** (1–3), 564–572. https://doi.org/10.1016/j.jhazmat.2010.03.041.

Senol, Z. M. 2020 Effective biosorption of Allura red dye from aqueous solutions by the dried-lichen (*Pseudoevernia furfuracea*) biomass. *International Journal of Environmental Analitycal Chemistry*. https://doi.org/10.1080/03067319.2020.1785439.

Sinetova, M. A., Bolatkhan, K., Sidorov, R. A., Mironov, K. S., Skrypnik, A. N., Kupriyanova, E. V., Zayadan, B. K., Shumskaya, M. & Los, D. A. 2017 Polyphasic characterization of the thermotolerant cyanobacterium *Desertifilum* sp. strain IPPAS B-1220. *FEMS Microbiology Letters* **364** (4), 1–10. https://doi.org/10.1093/femsle/fnx027.

Tastan, B. E. & Tekinay, T. 2016 A novel coal additive from microalgae produced from thermal power plant flue gas. *Journal of Cleaner Production* **133**, 1086–1094. https://doi.org/10.1016/j.jclepro.2016.06.053.

Tastan, B. E., Tekinay, T., Celik, H. S., Ozdemir, C. & Cakir, D. N. 2017 Toxicity assessment of pesticide triclosan by aquatic organisms and degradation studies. *Regulatory Toxicology and Pharmacology* **91**, 208–215. https://doi.org/10.1016/j.yrtph.2017.10.030.

Theivandran, G., Mohamed, I. S. & Murugan, M. 2015 Fourier transform infrared (Ft-IR) spectroscopic analysis of *Spirulina fusiformis*. *Journal of Medicinal Plants Studies* **3**, 30–32.

Töre, Y., Ustaoğlu, F., Tepe, Y. & Kalipci, E. 2021 Levels of toxic metals in edible fish species of the Tigris River (Turkey); threat to public health. *Ecological Indicators* **123**, 107361.

Uzcan, F. & Soylak, M. 2020 Spectrophotometric determination of traces allura red in environmental samples after a deep eutectic solvent-based microextraction. *International Journal of Environmental Analytical Chemistry*, 1–11. https://doi.org/10.1080/03067319.2020.1738422.

First received 1 October 2021; accepted in revised form 26 November 2021. Available online 9 December 2021